Size to density coupling of supported metallic clusters

Elad Gross and Micha Asscher*

Received 4th June 2008, Accepted 24th October 2008
First published as an Advance Article on the web 26th November 2008
DOI: 10.1039/b809355e

One of the difficulties in standard growth of metallic nano-clusters on oxide substrates as model catalysts is the strong coupling between clusters size and density. Employing multiple cycles, amorphous solid water–buffer layer assisted growth (ASW-BLAG) procedure, we demonstrate how the size to density coupling can be eliminated under certain conditions. In this study, gold clusters were deposited on a SiO_2/Si(100) substrate in UHV, using ASW as a buffer layer assisting aggregation and growth. The clusters were imaged *ex situ* by tapping mode atomic force microscope (AFM) and high-resolution scanning electron microscope (HR-SEM). *In situ* Auger electron spectroscopy (AES) measurements have led to independent evaluation of the gold covered area. In order to increase the clusters density we have introduced a multiple BLAG procedure, in which, a BALG cycle is repeated up to 10 times. The cluster density can be increased this way by more than five fold without changing their size. Above a specific number of cycles, however, the cluster density reaches saturation and a gradual increase in clusters size is observed. Larger clusters correlate with lower saturation density following multiple BLAG cycles. This observation is explained in terms of long range cluster–cluster attraction between clusters already on the substrate and those approaching in the next BLAG cycle. This attraction is more pronounced as the clusters become larger. We have shown that at saturation density, inter-cluster distance can not be smaller than 20 nm for clusters 4 nm in diameter or larger. Employing two consecutive BLAG cycles, characterized by different parameters (metal dosage and buffer layer thickness) result in a bi-modal size distribution. Moreover, it is demonstrated that one can prepare this way co-adsorbed bi-metallic film of *e.g.* Au and Pd clusters, with specific density and size on the same substrate. The ASW-BLAG procedure is thus expected to introduce a new pathway for tailor made, versatile model catalysts.

1. Introduction

The catalytic activity of metallic clusters often depends on their morphology and size.[1–5] This explains the growing interest in the development of preparation methods of clusters with controlled morphologies, leading to better understanding of (clusters) structure–(catalytic) reactivity relations.[6–9] A typical model study of heterogeneous catalysis involves direct deposition (DD) of metal atoms onto oxide substrates. Diffusion and aggregation of the impinging metal atoms on a substrate lead to the formation of metallic clusters.[1–3,10,11] An alternative method in which the metal atoms are deposited on top of a cold buffer layer has been introduced by Huang *et al.*[12] In this method a chemically inert buffer layer separates the deposited (hot) metal atoms from the (cold) oxide substrate. Local coalescence of the metal atoms leads to the formation of small seed clusters on top of the buffer layer. Subsequent annealing of the sample leads to desorption of the buffer material, followed by aggregation and growth of the metal clusters *via* a buffer layer assisted growth (BLAG) mechanism. A variety of atoms and molecules have already been used as buffer material for assisting metal clusters growth. This includes Xe, Ar, Kr, CO_2 and H_2O.[13–19] The concept of weakly bound inert buffer layer was recently used for clusters[20] and thicker metallic films patterning[21] by employing laser ablation.

The size and density of clusters prepared by the DD method depend on the metal dosage, the substrate's temperature and the nature of the support.[1–5] In the case of BLAG procedure clusters size and density also depend on the metal dosage, however, here the buffer layer thickness becomes critically important.[12–18] Another difference is found in the clusters morphology. DD clusters are rather flat and characterized by an aspect ratio (height to diameter ratio) of $\sim$0.2 (in the case of gold clusters), while BLAG clusters (BC) are more hemispherical and have aspect ratio approaching $\sim$0.5. For a given metal dosage DD clusters are smaller and denser than BC.[16,19] Thicker buffer layer leads to the formation of BC characterized by larger aspect ratio. It was shown that gold dosage of 5 Å result in the formation of elongated and branched clusters, while hemispherical clusters are obtained at lower dosage of 1–2 Å Au.[13,14]

CO-IRAS (infrared reflection absorption spectroscopy) measurements revealed that CO molecules adsorbed on both DD and BLAG clusters are characterized by a single frequency of $\sim$2106 cm^{-1}. Even though DD clusters density is higher than the BC, the IRAS peak area of both types of clusters was similar. CO-TPD (temperature programmed

Department of Physical Chemistry and the Farkas Center for Light Induced Processes The Hebrew University of Jerusalem, Jerusalem, 91904, Israel. E-mail: Asscher@fh.huji.ac.i

desorption) measurements have shown that CO desorption profiles were similar for CO molecules adsorbed on the different clusters. CO-TPD peak temperature, however, was higher for DD clusters than for the BC.[22] This means stronger binding sites thought to be associated with metal atoms at the perimeter having some interaction with the substrate as is the case of the DD clusters.

Since the catalytic reactivity of small gold clusters was suggested to correlate with the fraction of surface gold atoms having low coordination number,[6,7] an increase in the clusters density should lead to a corresponding increase in the reaction rate and yield. The density of DD clusters grows by increasing the metal dosage, however it results in simultaneous increase in the clusters size which can modify their catalytic activity.[2,3,9] The same correlation between clusters density and their size has been demonstrated for a single BLAG cycle.[12–16]

In order to overcome this obstacle we have introduced the multiple-BLAG procedure for the first time in a previous work where the emphasis was on IR measurements of adsorbed CO molecules on the gold clusters.[22] In this article we focus on the multiple BLAG process. The correlation between the gold dosage on top of ASW layer and the multiple BLAG clusters morphology and density are characterized. In addition the parameters and limits of the multiple-BLAG procedure and the approach to saturation clusters density are discussed.

2. Experimental

Gold clusters were grown on SiO_2/Si(100) under UHV (ultra high vacuum) conditions (1×10^{-9} torr) and were characterized *in situ* by Auger electron spectroscopy (AES) and *ex situ* by atomic force microscopy (AFM) and high resolution scanning electron microscopy (HR-SEM). The SiO_2/Si(100) samples were clamped to a stainless steel foil connected to liquid nitrogen dewar *via* copper feedthroughs and two tantalum rods. A W26%Re–W5%Re thermocouple was spot welded to the back side of the stainless steel foil. Ar^+ ions were used to sputter clean the SiO_2 surface from (mostly) carbon contaminants, while the surface cleanliness was subsequently verified by AES. Triple distilled H_2O were introduced by backfilling the UHV chamber, adsorbing as amorphous solid water (ASW) on the sample at 120 K. Gold atoms were evaporated on top of the ASW layer in vacuum by a resistively heated tungsten filament (0.25 mm wire diameter) wrapped around a 1 mm diameter Au wire. Gold flux was calibrated utilizing an *in situ* quartz-microbalance (QMB), employing fixed deposition rates of 0.02 Å s^{-1}. The sample was heated to 300 K at a rate of 2 K s^{-1} following the metal deposition step, in order to remove the water layer. Aggregation and growth of the gold nano-clusters during the buffer layer evaporation result in deposition of the clusters on the SiO_2/Si(100) substrate. Electron beam energy of 2 KeV was used in order to measure Auger signals of silicon (KLL) at 82 eV and gold (MNN) at 48 eV employing a mini double pass CMA (LK-3000 model).

The sample was subsequently removed from the vacuum chamber, in order to image the metallic clusters in air by AFM and HR-SEM, at room temperature. Details on the BLAG method employing ASW as the buffer layer, clusters size distributions and densities obtained *via* a single cycle BLAG were reported elsewhere.[16]

In order to obtain atomic resolution imaging of the metallic clusters, the BLAG prepared Au and Pd clusters were grown using the same procedure mentioned above, on top of a standard transmission electron microscope (TEM) grid, composed of amorphous carbon film. These samples were subsequently removed from the UHV chamber and imaged at room temperature with a high resolution transmission electron microscope (HR-TEM) (Tecnai F20 G^2, line resolution 0.1 nm).

3. Results and discussion

3.1 BLAG clusters density

A brief summary of results obtained *via* a single BLAG cycle is given here as a reference for the multiple-BLAG procedure which follows. BLAG clusters (BC) can be prepared in different sizes and densities according to the metal dosage and the buffer layer thickness.[12–19] For example, 0.2 Å Au (as determined by QMB) on top of 100 monolayers (ML) of ASW result in clusters with average height and density of 1.2 nm and 8×10^{10} cm^{-2}, respectively. The clusters grown this way appear mostly as symmetric hemispherical objects, as imaged by *e.g.* HR-SEM (Fig. 1a). Increasing the gold dosage from 0.2 Å to 1 Å has led to larger clusters and higher density (Fig. 1b). Gold dosage of 2.5 and 3.5 Å (Fig. 1c and d, respectively) further increased the clusters size, however, the clusters density turned over and started to decrease. Moreover, clusters prepared by evaporation of 2.5 Å Au (and above) on 100 ML ASW form very different morphology, mostly elongated, often curved and branched objects. AFM analysis has led to the conclusion that these objects are composed from a few small clusters that have aggregated, but not fully fused together. In contrast, BLAG clusters that were prepared by less than 1.5 Å Au were nicely fused. These changes in clusters morphology as the metal dosage is increased were previously reported by Haley *et al.* (who employed rare gases as the buffer material).[13]

Fig. 2 summarizes the clusters density and height dependence on gold dosage on top of 100 ML ASW. Different behavior has been observed below and above equivalent dosage of 0.7 Å Au. Increasing the gold dosage (up to 0.7 Å) results in monotonic increase of both clusters size and

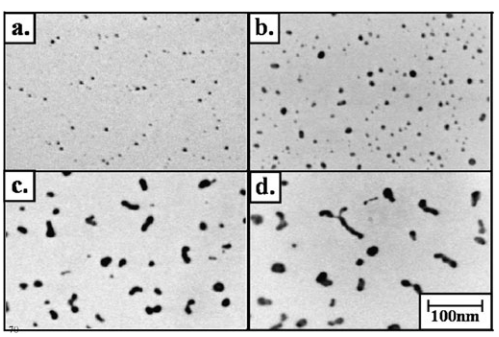

Fig. 1 HR-SEM images of gold clusters prepared by evaporation of 0.2 (a), 1 (b), 2.5 (c) and 3.5 Å Au (d) on 100 ML ASW.

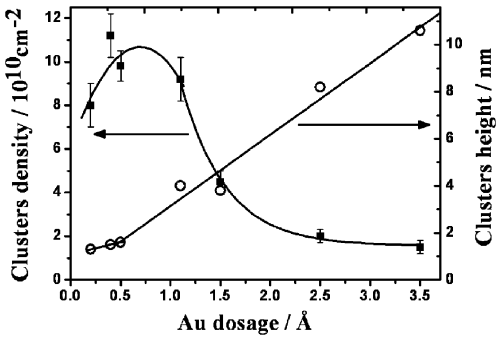

Fig. 2 Gold clusters density and height changes with gold dosage, as determined by QMB measurements. The gold clusters were prepared *via* BLAG, over 100 ML ASW.

density. This observation is anticipated, since it should lead to higher density of seed clusters on top of the ASW buffer layer. Higher density of seed clusters transform into higher density of large clusters on the silica surface, after the buffer layer has desorbed. However, when the gold dosage increases above 0.7 Å, bigger clusters at lower densities were formed. At this point the clusters were large enough to interact with each other leading to higher aggregation rate of the clusters. Clusters size (height) more rapidly increases for gold dosage above 0.7 Å (Fig. 2). Similar results were also observed for gold clusters deposited on top of 10 ML ASW (not shown).

Since clusters size and density were all determined by *ex situ* HR-SEM imaging, we have performed *in situ* AES measurments as a calibration of the total gold dosage. In particular, since both AFM and HR-SEM are not sensitive to very samll clusters and single atoms, AES can be rather valuable for elimination of the possibility that very small clusters can grow *via* BLAG. This may be a problem if the growth is over very thin buffer layer and at low substrate temperature. The Si (KLL) AES signal measured at 82 eV, shown in Fig. 3, reveals its dependence on gold dosage for clusters that were prepared by four different buffer layer thicknesses. As more gold is deposited, the clusters size and density also increase, as discussed above, leading to diminishing Si (KLL) AES signal

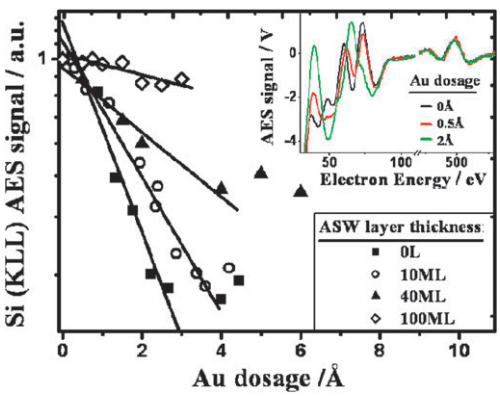

Fig. 3 Si (KLL) AES signal at 82 eV as a function of gold dosage. The gold clusters were prepared by evaporating different amounts of gold on 0, 10, 40 and 100 ML ASW on SiO_2/Si(100) followed by annealing to 300 K. Inset: AES of gold clusters on SiO_2/Si(100). The gold clusters were prepared by evaporation of 0, 0.5 and 2 Å Au on 10 ML ASW.

with simultaneous increase of the Au (MNN) signal (at 48 eV)[23] (Fig. 3, inset). The slopes of the plots that pertain to 0, 10, 40 and 100 ML ASW layer thicknesses were −0.3, −0.2, −0.09 and −0.01 $Å^{-1}$, respectively. The different slopes correspond to the various densities of BLAG clusters. For example, increasing the gold dosage on top of 10 ML ASW from 0.2 Å to 2 Å has doubled the clusters density, from 30×10^{10} cm^{-2} to 70×10^{10} cm^{-2}. This has led to a corresponding decay of the Si (KLL) AES signal to half of its value for clean SiO_2/Si(100). In contrast, when the same gold dosage was deposited on top of 100 ML ASW, the actual gold coverage has increased from 0.003 ML (cluster radius = 1.3 nm, density = 8×10^{10} cm^{-2}) to 0.04 ML (cluster radius = 6.5 nm, density = 3×10^{10} cm^{-2}), leaving 96% uncovered Si area, consistent with the data in Fig. 3 diamond symbols.

The density of clusters prepared by direct deposition (DD) is higher than the equivalent BLAG clusters and their aspect ratio (height to diameter ratio) is smaller, leading to more effective Si AES signal blocking by the deposited gold.[16,19] This is manifested in Fig. 3 (largest slope, solid squares).

We conclude that clusters of average size larger than 3 nm prevent further increase of density, regardless of the buffer thickness. This is attributed to inter-clusters attraction, to be further discussed in section 3.2 below.

3.2 Multiple-BLAG clusters

High density of nanometer size metallic clusters on oxide support is essential for improved sensitivity, yield and selectivity studies of model catalysis. Any attempt to increase the clusters density by raising the gold dosage is associated with modification in clusters size and shape. Achieving the goal of clusters density increase with only minor changes in clusters dimensions is demonstrated here by introducing the multiple BLAG concept. The BLAG procedure was repeated as many as ten times on the same substrate by employing identical parameters (buffer layer thickness and gold dosage) in order to increase the clusters densities. When 0.5 Å Au was deposited on 40 ML of ASW, the sample obtained this way was characterized by clusters density and height of $(18 \pm 3) \times 10^{10}$ cm^{-2} and 1.3 ± 0.2 nm, respectively (Fig. 4a). Repeating the same procedure for seven times has led to clusters density and height of $(98 \pm 7) \times 10^{10}$ cm^{-2} and 1.6 ± 0.4 nm, respectively (Fig. 4b). The clusters density has increased by more than five fold, while their height has increased only by 30%. Up to seven BLAG cycles the clusters density increases almost linearly, associated with only minor changes in clusters height (Fig. 4c). Inspection of the height distribution of clusters prepared by one and seven cycles reveals that it became wider as the number of cycles increased (Fig. 4d). The FWHM (full width at half maximum) values of a Gaussian fit to the clusters height distributions were 1.0 and 1.2 nm for one and seven cycles, respectively. When the number of cycles was further increased from seven to ten, the clusters density reached saturation values. Consequently, the cluster height started to increase faster.

Samples prepared by deposition of 0.5 Å gold on 100 ML ASW are characterized by clusters density and height of (9 ± 2) 10^{10} cm^{-2} and 1.5 ± 0.3 nm (Fig. 5a). Repeating this

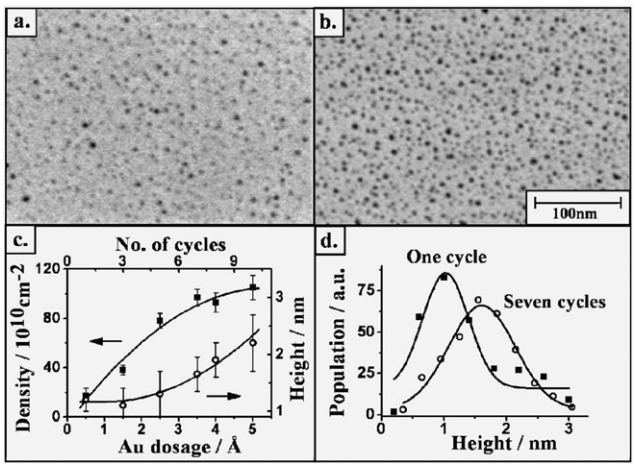

Fig. 4 HR-SEM images of gold clusters prepared by one (a) and seven (b) cycles of 0.5 Å Au evaporated on 40 ML ASW followed by annealing to 300 K. The dependence of gold dosage on clusters size and density is shown in (c). Cluster height distributions and their Gaussian fit are presented (d) for clusters shown in (a) and (b).

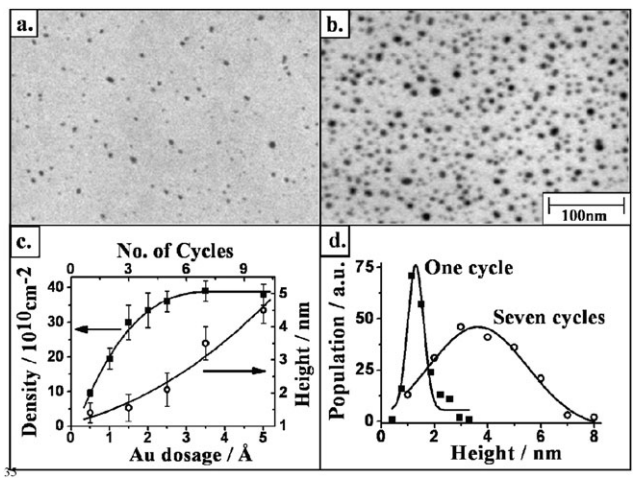

Fig. 5 HR-SEM images of gold clusters prepared by one (a) and seven (b) cycles of 0.5 Å Au evaporated on 100 ML ASW followed by annealing to 300 K. The dependence of gold dosage on clusters size and density is shown in (c). Cluster height distributions and their Gaussian fits are presented (d) for clusters shown in (a) and (b).

procedure for seven times results in clusters density and height of (38 ± 5) 10^{10} cm^{-2} and 3.5 ± 0.5 nm (Fig. 5b). Here, the clusters density increased by a factor of four, and their height has increased more than twice. In this case, the multiple-BLAG procedure has led to changes in both clusters size and density. Up to three cycles, the density increase was almost linear, while the clusters size stayed almost unchanged. More cycles results in gradual increase in clusters size with practically no change in density (Fig. 5c). The FWHM values of a Gaussian fit to the clusters height distributions is 1 and 4.4 nm for one and seven cycles, respectively (Fig. 5d).

Following seven cycles, the widths of the clusters height distributions obtained from buffer layer thicknesses of 40 and 100 ML ASW, have increased by a factor of 1.1 and 4.4, respectively, compared to the distribution obtained by a single BLAG cycle. This is predominantly due to growing weight of large clusters in their size distribution.

The significant effect of the buffer layer thickness on size distribution originates from attractive interactions among the clusters. This dominates the aggregation and growth of the clusters during evaporation–desorption of the buffer material. The longer aggregation time available during evaporation of thicker buffer layer, enables formation of significantly larger clusters, yet retaining also smaller ones. This results in an overall wider distribution of clusters sizes. How effective is the aggregation and growth of the metallic clusters during the window of time in which the buffer material evaporates, strongly depends on the nature of long range attraction between the growing metallic clusters. Such attraction is predicted to correlate with the metallic cohesive energy.[14]

The MC-BLAG procedure enables one to address the following question: Is there a correlation between the (average) nearest neighbor clusters center-to-center distance (r_{av}) observed at saturation density and the average cluster size, following ***n*** BLAG cycles. The minimum distance (r_{av}) was determined experimentally from HR-SEM images, deriving the average distance between clusters along 20 random lines, each was 500 nm long. This procedure was repeated for each of the images relevant to the samples discussed in Table 1 below.

An apparent correlation is observed, whereby the average distance r_{av} at saturation density, increases with the average cluster size, obtained at thicker ASW layer. The average distance (r_{av} in Table 1) has doubled by increasing the buffer thickness from 40 ML to 100 ML ASW. This conclusion suggests that the larger clusters interact attractively more strongly, over a longer distance with those clusters that are descending towards the substrate upon desorption of the buffer layer in the next BLAG cycle. This typically results in saturation cluster density at smaller number of BLAG cycles for the larger clusters obtained with thicker buffer layers. It is interesting to note that average inter-clusters distance between nearest neighbors as long as 24 nm (distance between nearest-neighbor clusters' perimeters of 20 nm) does not allow an extra cluster to land in between even though the descending (average) cluster diameter is only about 4 nm. BLAG cycles above the number which leads to saturation density, result in a gradual increase of the clusters size without further change in density, as discussed above.

The density of BLAG clusters prepared by buffer layer thickness of 100 ML reached saturation value already after three cycles. One way to explain a constant density of clusters is diffusion and coalescence of clusters arriving later with those that have already been deposited on the surface.

This, however, is less likely to occur upon annealing to 300 K. HR-SEM images of samples annealed in vacuum to 400 K prior to imaging have shown no change in size and density. This was the case particularly for larger clusters (100 ML buffer thickness) since the larger clusters are known to diffuse more slowly than smaller ones.[20]

Therefore, the density of clusters stays almost unchanged while the clusters size rapidly increases with each extra BLAG cycle upon their coalescence. In contrast, thinner buffer layers lead to the formation of smaller clusters. Shorter period of

Table 1 Summary of multi-cycle BLAG clusters parameters

ASW thickness (ML)	Au dosage/Å	r_{av}/nm	d_{av}/nm	σ ($\times 10^{10}$)/cm^2	n
10	0.5	8.6 ± 1	2.1 ± 0.3	130 ± 10	3
40	0.5	11.6 ± 1	3.5 ± 0.2	98 ± 7	6
100	0.5	24.7 ± 4	4.1 ± 2.5	38 ± 5	4
100	1.5	34 ± 5	12 ± 5.6	15 ± 4	3

r_{av} = average center to center distance of nearest neighbour clusters at saturation density; d_{av} = average cluster diameter at saturation coverage; σ = saturation density (clusters cm^{-2}); n = number of BLAG cycles.

elapsed time till clusters arrive and stick to the substrate, prevents lateral diffusion and aggregation, during the buffer evaporation. This allows for more cycles and higher densities while the clusters size is kept almost constant. An exception is the case of the thin buffer layer of 10 ML, where relatively high density of small clusters (about 2 nm diameter) are formed already in the first BLAG cycle. As a result, the maximum achievable saturation density of 130×10^{10} clusters cm^{-2} is reached following 3 BLAG cycles.

Increasing the total coverage of clusters as a result of multiple BLAG can be monitored by measuring the Si (KLL) AES (at 82 eV) signal intensity *vs.* the number of BLAG cycles, in a similar way to the effect discussed for a single BLAG cycle in Fig. 3. This is shown for ASW layer thicknesses of 40 and 100 ML (lines A and B in Fig. 6, respectively). Clusters prepared from buffer layer thickness of 40 ML ASW are denser than those prepared on top of 100 ML, therefore, the silicon AES signal decays faster, as discussed in Fig. 3. It should be noted that after ~6 cycles the slope of curve B gradually levels off. These results are in good agreement with the clusters density graph (Fig. 5), where at this point the clusters density reaches saturation. Only minor changes are threfore expected and actually observed in the silicon AES signal as the clusters continue to grow (Fig. 6B).

Since clusters density increases during the initial BLAG cycles, the silicon Auger signal obtained from these samples decays faster than that from a single BLAG at the same total gold dosage. Analysis of HR-SEM images have confirmed that increasing the gold dosage by several consecutive cycles results in larger gold covered area than for single BLAG cycle with identical gold dosage (Fig. 6, inset).

From the AES data we may conclude that within our experimental uncertainty, no single atoms or clusters smaller than 0.5 nm are formed during the BLAG procedure. It is important to note that this conclusion can be obtained only if the same sample is analyzed first *in situ via* AES and subsequently *ex situ* using the clusters imaging methods, as demonstrated above.

3.3 Bi-modal size distribution

The multiple-BLAG procedure enables one to prepare clusters at different sizes and densities on the same substrate. In each cycle the BLAG parameters, namely the gold dosage and buffer layer thickness, should fit the desired clusters density and size. HR-SEM image of a sample composed of two consecutive but different BLAG cycles is shown in the inset of Fig. 7. 0.5 Å Au were deposited first on 20 ML ASW followed by slow annealing to 300 K. Subsequently, 1.7 Å Au was deposited on the same sample on top of 100 ML ASW with subsequent annealing to 300 K.

The sample clearly contains two different average cluster sizes, as indicated in Fig. 7. The small clusters are characterized by average height and density of 0.9 ± 0.2 nm and 45×10^{10} cm^{-2}, respectively. The larger clusters height and density are 6 ± 2 nm and 3×10^{10} cm^{-2}, respectively. The clusters size and density of each of the different BLAG cycles

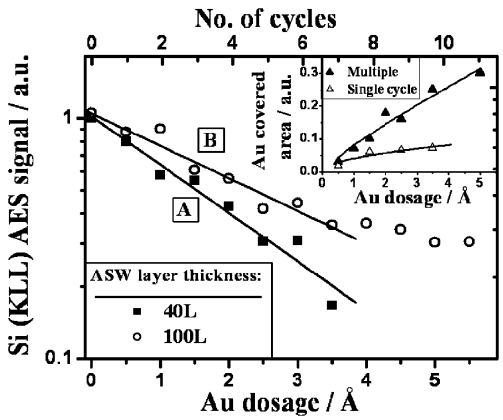

Fig. 6 Si (KLL) AES signal at 82 eV as a function of BLAG cycles and total gold dosage. In each BLAG cycle gold clusters were prepared by evaporating 0.5 Å on 40 ML (A) and 100 ML (B) ASW on SiO_2/Si(100). Annealing to 300 K separate between the cycles. Inset: gold covered area (as analyzed from HR-SEM measurements) as a function of gold dosage. The clusters were prepared by single and multiple BLAG cycles, over 100 ML ASW as the buffer layer.

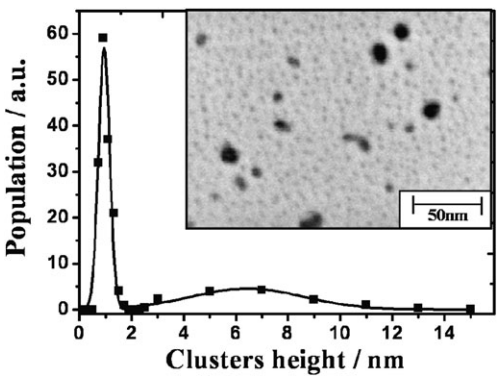

Fig. 7 Gold clusters height distribution and their Gaussian fit. These bi-modal gold clusters were prepared by two consecutive BLAG cycles. The clusters were prepared by evaporation of 0.5 Å Au on 20 ML ASW followed by evaporation of 1.7 Å Au on 100 ML ASW, between the cycles the sample was annealed to 300 K. Inset: HR-SEM image of the gold clusters prepared by the two different BLAG parameters.

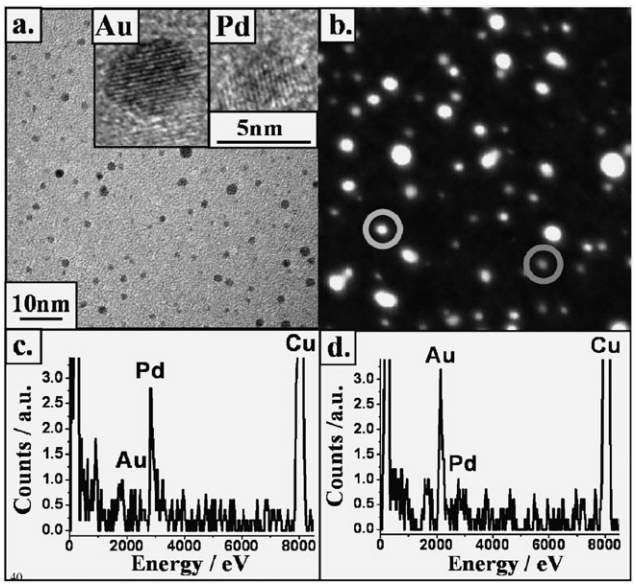

Fig. 8 HR-TEM image of gold and palladium clusters deposited on amorphous carbon film. The clusters were prepared by evaporation of 0.5 Å Pd on 100 ML ASW followed by evaporation of 0.5 Å Au on 100 ML ASW. Between the cycles the sample was annealed to 300 K. Inset: magnification of Au and Pd clusters, the lattice structure can be clearly resolved (a). STEM image of the same sample is shown in (b). EDS of the red circled and grey circled clusters are shown in (c) and (d), respectively.

are equivalent to those of the corresponding single BLAG cycle with identical parameters. We may conclude, therefore, that in the bi-modal BLAG sample, the clusters prepared in the first cycle do not modify the subsequent deposition cycles. This is true as long as the density is far enough from saturation.

3.4 Bimetallic BLAG

The multiple BLAG procedure enables us yet another unique advantage: different metal elements can be grown on the same substrate at different sizes and densities. As an example, gold and palladium clusters were prepared this way by having a first BLAG cycle composed of 0.5 Å Pd on 100 ML ASW, followed by a second cycle in which 0.5 Å Au were deposited on identical buffer thickness.

Due to the difference in the atomic number of Pd and Au (46 and 79, respectively), one can clearly distinguish between the bright palladium and the darker gold clusters obtained in the HR-TEM image (Fig. 8a). The different metal clusters can be distinguished also by their lattice constant once imaged on the carbon substrate as a mono-crystallite. In the inset of Fig. 8 the lattice structure of gold and palladium crystallites is viewed. The atom resolved data enables the measurement of inter-planes distance of gold and palladium nano-crystals that are 2.37 Å and 2.23 Å, respectively. This is obtained *via* standard fast Fourier transform (FFT) analysis of the data. The FFT results verify that these clusters are oriented predominantly along the (111) crystallographic orientation. Scanning TEM (STEM) image of the same sample is sohwn in Fig. 8b. In this scan mode the gold clusters are much brighter than the palladium clusters. Energy dispersion spectra of the X-ray emitted from palladium (dark spot, red circled) and gold (bright spot, grey circled) clusters are shown in Fig. 8c and d, respectively. These measurements verify that each of the clusters is monometallic.

4. Conclusions

Amorphous solid water layers were utilized to assist the growth (BLAG) of gold nano-clusters. Their morphology was examined as a function of gold dosage. Increasing the gold dosage above 2 Å has led to clusters density decrease followed by a change in clusters morphology. Above this point the typically hemispherical BLAG clusters become elongated, constructed from a few clusters that have not been fully fused together. Any attempt to increase the BLAG clusters density by increasing the gold dosage would lead to changes in the clusters morphology. The density of BLAG and directly deposited (DD) clusters is coupled to their size and one cannot simply separate these two parameters. In order to overcome this obstacle and be able to decouple the BLAG clusters density and size (within a limited density range), we have introduced the multiple-BLAG procedure. This procedure enables one to increase the BLAG clusters density up to five fold with only minor changes in clusters size. This is however limited to buffer layers thinner than 50 ML and relatively small dosage of the deposited metal, below 0.5 Å. It is demonstrated that thicker buffer layers tend to limit the maximum possible density. Due to effective aggregation during the (longer) buffer evaporation time, their density would reach saturation at smaller number of BLAG cycles. A correlation was found between the clusters size and saturation density with minimum inter-clusters distances of 20 nm at saturation coverage of clusters larger than 4 nm in diameter.

In addition to bi-modal clusters size distribution, metal clusters from different elements were grown using the multiple-BLAG method. We have shown that one can prepare a sample containing Pd and Au clusters at specific sizes and densities on the same substrate by two consecutive BLAG cycles. Catalytically active metal clusters can thus be prepared on the same substrate with optimum size for a specific reaction.

Acknowledgements

This research was partially supported by a grant from the US-Israel Binational Science Foundation, by the Israel Science Foundation and the German-Israel Foundation. The Farkas center is supported by the Bundesministerium fur Forschung und Technologie and the Minerva Gesellschaft fur die Forschung mbh.

References

1 C. T. Campbell, *Surf. Sci. Rep.*, 1997, **27**, 1.
2 C. R. Henry, *Surf. Sci. Rep.*, 1998, **31**, 231.
3 M. Bäumer and H. J. Freund, *Prog. Surf. Sci.*, 1999, **61**, 127.
4 M. Haruta, *Catal. Today*, 1997, **36**, 153.
5 M. Valden, X. Lai and D. W. Goodman, *Science*, 1998, **281**, 1647.
6 N. Lopez, T. V. W. Janssens, B. S. Clausen, Y. Xu, M. Mavrikakis, T. Bligaard and J. K. Nørskov, *J. Catal.*, 2004, **223**, 232.

7 T. V. W. Janssens, B. S. Clausen, B. Hvolbæk, H. Falsig, C. H. Christensen, T. Bligaard and J. K. Nørskov, *Top. Catal.*, 2007, **44**, 15.
8 M. S. Chen and D. W. Goodman, *Acc. Chem. Res.*, 2006, **39**, 739.
9 M. S. Chen and D. W. Goodman, *Catal. Today*, 2006, **111**, 22.
10 A. Kolmakov and D. W. Goodman, *Chem. Rev.*, 2002, **2**, 446.
11 X. Lai, T. P. St Clair, M. Valden and D. W. Goodman, *Prog. Surf. Sci.*, 1998, **59**, 25.
12 L. Huang, S. J. Chey and J. H. Weaver, *Phys. Rev. Lett.*, 1998, **80**, 4095.
13 C. Haley and J. H. Weaver, *Surf. Sci.*, 2002, **518**, 243.
14 V. N. Antonov, J. S. Palmer, A. S. Bhatti and J. H. Weaver, *Phys. Rev. B*, 2003, **68**, 205418; V. N. Antonov, J. S. Palmer, P. S. Waggoner, A. S. Bhatti and J. H. Weaver, *Phys. Rev. B*, 2004, **70**, 45406.
15 P. S. Waggoner, J. S. Palmer, V. N. Antonov and J. H. Weaver, *Surf. Sci.*, 2005, **596**, 12.
16 E. Gross, Y. Horowitz and M. Asscher, *Langmuir*, 2005, **21**, 8892.
17 E. Gross, O. Stein and M. Asscher, *Appl. Surf. Sci.*, 2007, **253**, 6545.
18 G. Liang and S. P. Perry, *Surf. Sci.*, 2005, **594**, 132.
19 X.-M. Yan, J. Ni, M. Robbins, H. J. Park, W. Zhao and J. M. White, *J. Nanopart. Res.*, 2002, **4**, 525.
20 G. Kerner, Y. Horowitz and M. Asscher, *J. Phys. Chem. B*, 2005, **109**, 4545.
21 G. Kerner and M. Asscher, *Nano Lett.*, 2004, **4**, 1433.
22 E. Gross, M. Lundwall, D. W. Goodman and M. Asscher, *J. Phys. Chem. C*, 2007, **111**, 16197.
23 K. Luo, D. Y. Kim and D. W. Goodman, *J. Mol. Catal. A*, 2001, **167**, 191.

